Pergamon

Ocean Engng, Vol. 22, No. 7, pp. 669–686, 1995

0029–8018/95 $9.50 + .00

0029–8018(95)00002-X

THE DETERMINATION OF CONFIDENCE LIMITS ASSOCIATED WITH ESTIMATES OF THE SPECTRAL PEAK FREQUENCY

I. R. Young

Department of Civil Engineering, University College, University of New South Wales, Canberra, ACT 2600, Australia

(*Received* 5 *August* 1994; *accepted* 5 *October* 1994)

Abstract—A Monte-Carlo simulation technique is used to evaluate the suitability of proposed techniques for the estimation of the spectral peak frequency. Due to the statistical variability of spectral estimates and the discrete frequency resolution of spectra, the calculated values of peak frequency are stochastic variables. The probability density functions for such estimates are functions of the frequency resolution and the number of degrees of freedom of the spectrum from which they are derived as well as the spectral peakedness. The mean values of all techniques are biased high, indicating the derived values of peak frequency are an overestimate of the true value. The probability density functions do not follow an obvious analytical form. Tabular values are, however, presented to enable the determination of confidence limits for estimates of the peak frequency.

1. INTRODUCTION

Wave spectra determined from the analysis of finite records of water surface elevation are subject to statistical uncertainty. This uncertainty occurs since the record has been truncated at some finite length. As a result, the derived spectrum is only an estimate of the "true" spectral form. The degree of uncertainty depends on the precise details of the processing used to determine the spectral estimate and is usually represented by the inclusion of confidence limits. Since the spectral estimate is a statistical quantity with an associated uncertainty, derived quantities such as significant wave height and the peak frequency will also be statistical variables. The determination of confidence limits for the significant wave height has been described previously. Knowledge of the statistical uncertainty associated with estimates of the peak frequency is, however, much poorer. This paper examines a number of methods for the determination of the peak frequency and utilizes a Monte-Carlo method for the determination of confidence limits associated with these estimates.

The arrangement of the paper is as follows. In Section 2 the theory governing the statistical variability of spectral estimates and quantities derived from spectral estimates is presented. This is followed in Section 3 by a review of different procedures proposed for the estimate of the peak frequency. The Monte-Carlo technique used to assess these various techniques and the confidence limits associated with the estimates are presented in Section 4. The conclusions follow in Section 5.

2. STATISTICAL VARIABILITY OF SPECTRAL ESTIMATES

For a stationary (ergodic) Gaussian process $x(t)$ (i.e. the water surface elevation), the variance spectrum is (Bendat and Piersol, 1971)

$$F(f) = 2 \lim_{T \to \infty} \frac{1}{T} E\,[|X(f,T)|^2] \tag{1}$$

where E indicates the expectation value; T is the length of the time series and $X(f,T)$ is the Fourier transform of the time series $x(t)$. An estimate of $F(f)$ can be obtained by simply omitting the limiting and expectation values in (1):

$$\hat{F}(f) = \frac{2}{T}|X(f,T)|^2 . \tag{2}$$

The resulting spectral estimate $\hat{F}(f)$ follows a chi-square probability distribution with $n = 2$ degrees of freedom (Bendat and Piersol, 1971):

$$\frac{\hat{F}(f)}{F(f)} = \frac{\chi_2^2}{2} . \tag{3}$$

The number of degrees of freedom in the spectral estimate $\hat{F}(f)$ can be increased by averaging neighbouring frequency bins (frequency averaging) or by averaging spectra obtained from a sub-divided time series (ensemble averaging) (Bendat and Piersol, 1971). If the resulting spectral estimate has n degrees of freedom, the confidence limits for this estimate become

$$\frac{n\hat{F}(f)}{\chi^2_{n;\alpha/2}} \leq F(f) < \frac{n\hat{F}(f)}{\chi^2_{n;1-\alpha/2}} \tag{4}$$

where $\chi^2_{n;\alpha}$ is the α percentage point of the chi-square distribution with n degrees of freedom. If, for example, the 95% confidence interval is required, then $(1 - \alpha) = 0.95$.

Donelan and Pierson (1983) and Young (1985) have shown that the variance as calculated from the integral of the spectrum also follows a chi-square distribution but with the number of degrees of freedom, ν, depending on the spectral shape:

$$\nu = \frac{n\left[\sum_{i=1}^{N} \hat{F}(f_i)\right]^2}{\sum_{i=1}^{N} [\hat{F}(f_i)]^2} . \tag{5}$$

Confidence limits for the significant wave height, H_s, based on the variance obtained from integration of $\hat{F}(f)$, become

$$\left[\frac{\nu}{\chi^2_{\nu;1-\alpha/2}}\right]^{1/2} \hat{H}_s \leq H_s < \left[\frac{\nu}{\chi^2_{\nu;\alpha/2}}\right]^{1/2} \hat{H}_s . \tag{6}$$

3. METHODS FOR ESTIMATING SPECTRAL PEAK FREQUENCY

A number of different methods have been proposed for the estimation of the spectral peak frequency from spectral estimates defined at discrete values of frequency. A number of these techniques will be described in this section, and a detailed assessment of their respective performance is contained in Section 4. The two major problems which arise in the accurate determination of f_p are: (i) the statistical variability of the spectral estimate and (ii) the finite and often coarse frequency resolution of the discrete spectrum.

3.1. *Simple maximum*

The most obvious and straightforward method for the determination of f_p is to simply select the frequency associated with the maximum spectral ordinate, $f_p^{\max}$.

3.2. *"Delft" method*

A method such as $f_p^{\max}$ is very susceptible to the effects of both sampling variability and finite spectral resolution. Such effects would be reduced by techniques which utilized multiple spectral bands in the determination of f_p. A number of such techniques have been proposed. The so-called "Delft" method (IAHR/PIANC, 1986; Mansard and Funke, 1988, 1990) involves the determination of the centroid of a spectral band about the maximum ordinate

$$f_p^{Dm} = \frac{\displaystyle\int_{f_1}^{f_2} f\,F(f)\mathrm{d}f}{\displaystyle\int_{f_1}^{f_2} F(f)\mathrm{d}f}. \tag{7}$$

The frequency thresholds f_1 and f_2 are chosen as the upper and lower frequencies at which the spectral energy is a fraction, m, of the maximum spectral ordinate, $F(f_p^{\max})$. Two commonly used thresholds are m = 80 and 60% (Mansard and Funke, 1990), giving rise to the estimates f_p^{D80} and f_p^{D60}, respectively.

3.3. *Weighted mean*

Sobey and Young (1986) and Reid (1986) have proposed a method involving a weighted mean over the whole spectrum rather than a partitioned region as in f_p^{Dm}. The weighting is biased towards the energetic portions of the spectrum

$$f_p^{Mq} = \frac{\displaystyle\int_0^{\infty} f\,F^q(f)\mathrm{d}f}{\displaystyle\int_0^{\infty} F^q(f)\mathrm{d}f}. \tag{8}$$

A variety of values for the weighting exponent, q, have been proposed. Sobey and Young (1986) proposed $q = 8$, giving rise to the estimate f_p^{M8}, whereas Reid (1986) proposed $q = 5$, yielding f_p^{M5}.

3.4. *Peak centroid*

A modification to the "Delft" method has been proposed by Günther (1981) and Bishop and Donelan (1988) (f_p^{PC}). Rather than defining upper and lower thresholds, they integrate over the three highest spectral bands. A further variation of this method would be to fit an interpolation spline to the ordinates of these three values. The maximum value of the spline provides an estimate of the peak frequency, f_p^S.

4. MONTE-CARLO SIMULATION

4.1. *Description of simulation method*

As noted above, the spectral estimate $\hat{F}(f)$ is a random variable following a chi-squared probability distribution with n degrees of freedom, χ_n^2. This variability leads to uncertainty in the determination of f_p by any of the above methods. Additional uncertainty is introduced, since ordinates of $\hat{F}(f)$ are available only at discrete values of f defined by the spectral resolution, Δf. Hence, the estimate of the peak frequency, $\hat{f}_p$, will be a random variable, the probability distribution of which will be a function of both n and Δf. A Monte-Carlo simulation method was adopted to account for the statistical variability of the spectral estimate introduced by these two factors.

A mean spectral form following that proposed by Donelan *et al.* (1985) was adopted:

$$F(f) = \alpha g^2(2\pi)^{-4} f_p^{-1} f^{-4} \exp\left[-\left(\frac{f}{f_p}\right)^{-4}\right] \cdot \gamma^{\exp\left[\frac{-(f-f_p)^2}{2\sigma^2 f_p^2}\right]}. \tag{9}$$

Typical spectral parameters of $\alpha = 0.01$, $\sigma = 0.07$ and $\gamma = 3.0$ were chosen. A total of 63 different combinations of normalized frequency resolution, $\Delta f/f_p$, and degrees of freedom, n, were investigated. The values utilized were: $\Delta f/f_p = 0.01, 0.05, 0.10, 0.15, 0.20, 0.25, 0.30, 0.35, 0.40$ and $n = 5, 10, 25, 50, 75, 100, 150$. For each of these 63 combinations of $\Delta f/f_p$ and n, 10,000 realizations of $\hat{F}(f)$ were generated from $F(f)$. For each realization, a discrete frequency grid was defined with a resolution, $\Delta f/f_p$. The first point in this grid was defined as $f_0/f_p = 0.2 + r\Delta f/f_p$, where r is a value between 0 and 1, selected from a uniformly distributed random number generator. At each ordinate of this discrete grid, $\hat{F}(f)$ was determined. Each of these values was evaluated independently from a chi-squared random number generator with mean $F(f)$ and n degrees of freedom. Hence, the discrete grid could vary in frequency space by $\Delta f/f_p$ and each ordinate of the spectrum would follow a χ_n^2 distribution.

For each realization of the spectrum, $\hat{F}(f)$, $\hat{f}_p$ was determined using the different techniques described above. For each method, the 10,000 values of $\hat{f}_p$ were sorted into ascending order and the values exceeded by 2.5% and 97.5% of the estimates were determined, thus defining the 95% confidence limits. The mean of the estimates was also determined.

4.2. *Probability density functions for estimates*

A total of eight different variations of the methods described in Section 3 were investigated. These were: the simple maximum, $f_p^{\max}$; the Delft method, f_p^{D60}, and f_p^{D80}; the weighted mean, $f_p^{M4}, f_p^{M5}, f_p^{M8}$; the weighted centroid, f_p^{PC}; and the spline method, f_p^S. From the Monte-Carlo simulations for each of these methods, the resulting probability density functions (pdfs) can be found as functions of $\Delta f/f_p$ and n. Examples of the pdfs for each of the four general methods discussed in Section 3 are shown in Fig. 1. Space limitations preclude showing all eight methods investigated. Also, only 20 of the total of 63 combinations of $\Delta f/f_p$ and n investigated for each method are

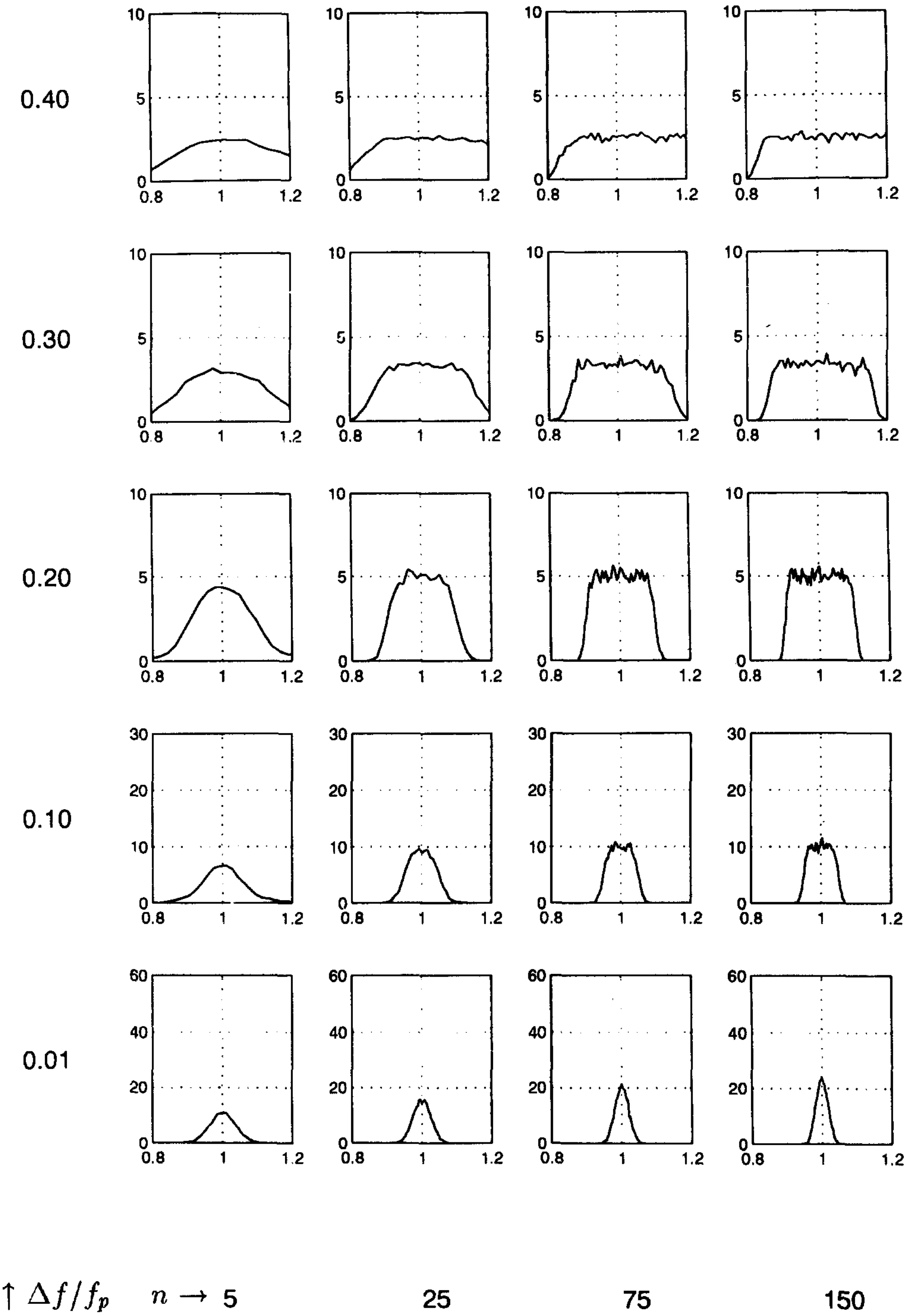

Fig. 1(a). Probability density functions for estimates of the peak frequency for the simple maximum method, f_p^{max} as a function of relative frequency resolution, $\Delta f/f_p$ and degrees of freedom, n. The horizontal axis on each panel is normalized frequency, f/f_p.

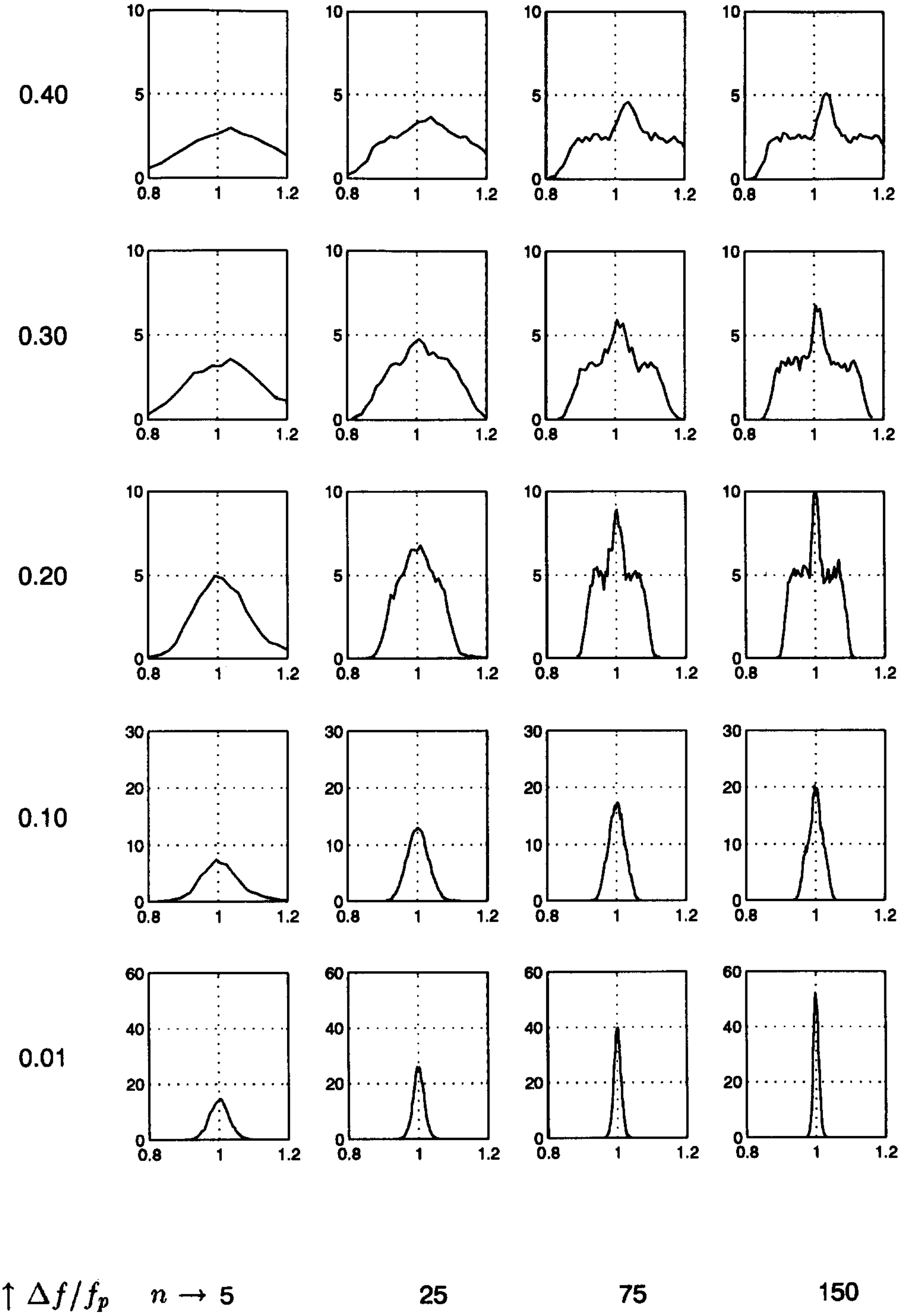

Fig. 1(b). As for Fig. 1(a), but for the "Delft" method, f_p^{D80}.

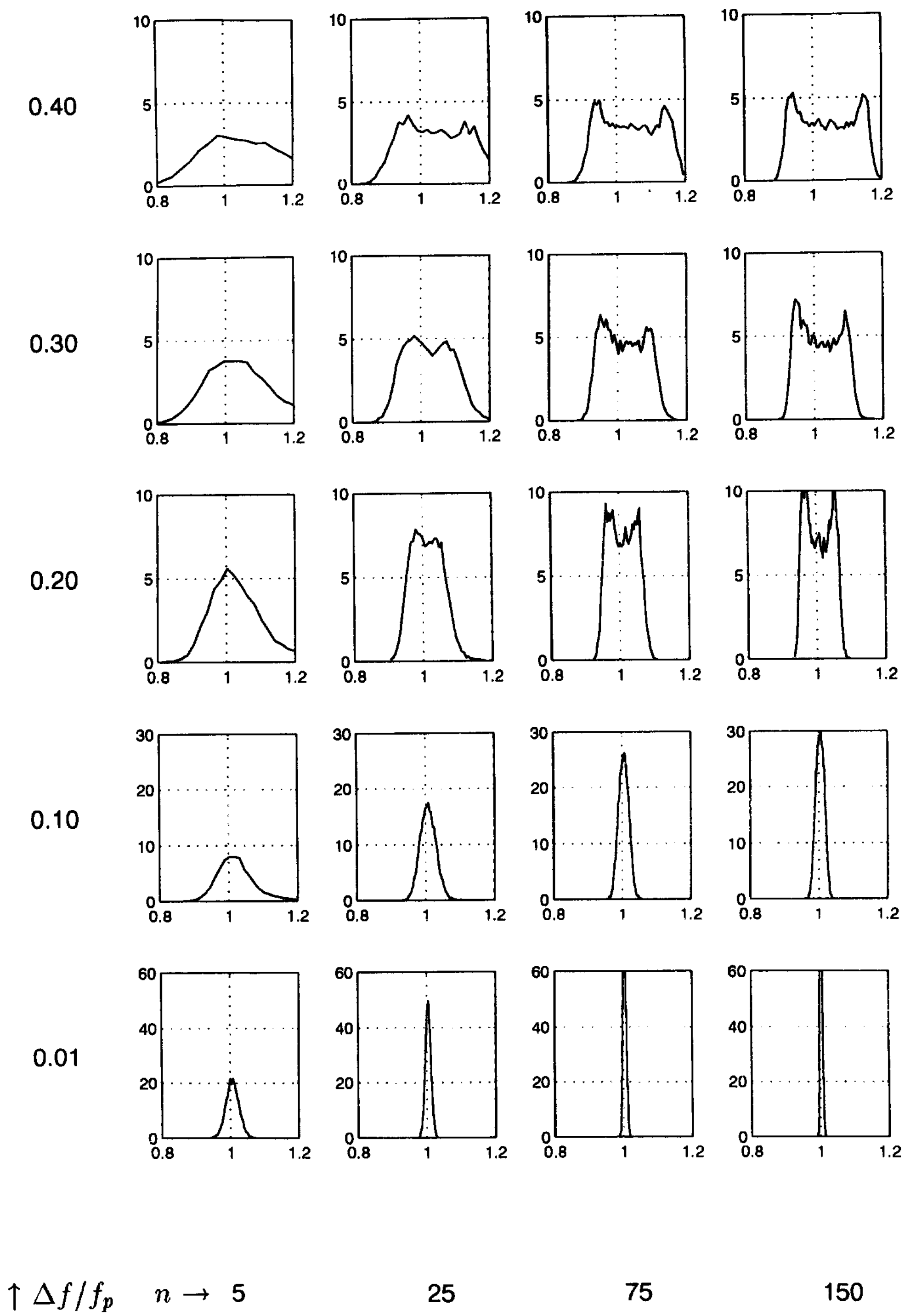

Fig. 1(c). As for Fig. 1(a), but for the weighted mean method, f_p^{M4}.

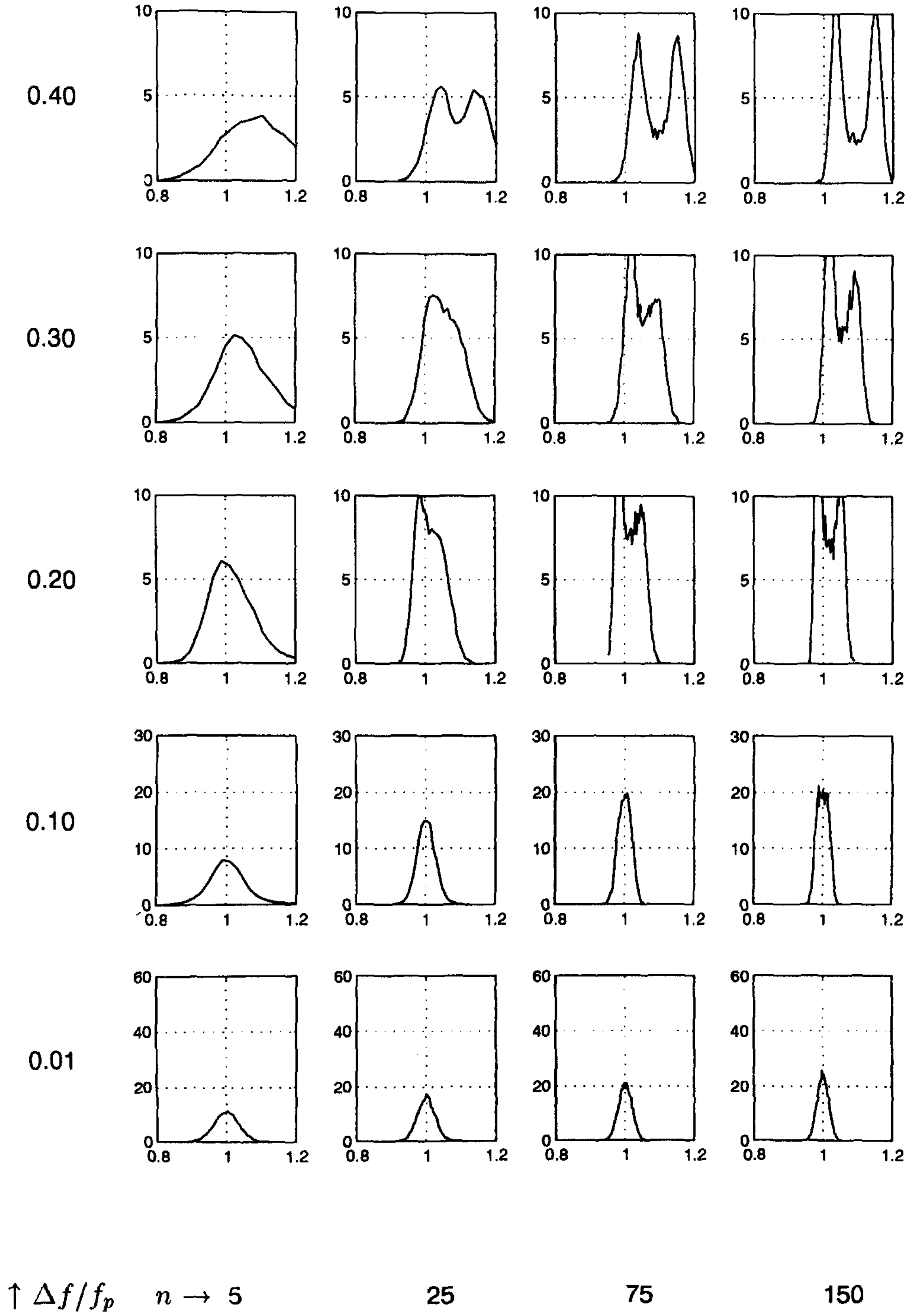

Fig. 1(d). As for Fig. 1(a), but for the peak centroid method, f_p^{PC}.

shown. Results for f_p^{max} [Fig. 1(a)], f_p^{D80} [Fig. 1(b)], f_p^{M4} [Fig. 1(c)] and f_p^{PC} [Fig. 1(d)] are shown.

The dual dependence of the pdfs on $\Delta f/f_p$ and n is clear from these figures. The shape of the pdfs vary both as a function of these quantities as well as between methods. A number of general trends are, however, clear. For small $\Delta f/f_p$ and large n the spectral resolution is high and there is little sampling variability in the spectral estimates. Hence, all methods provide unbiased estimates of f_p with little variability. That is, the pdfs are very peaked. They are also symmetric about the true value of f_p. As n decreases the pdfs become broader (i.e. the variance increases) but they remain symmetric about f_p. Provided $\Delta f/f_p$ remains small the pdfs approximate normal distributions, despite the fact that the individual spectral estimates from which they were calculated follow a χ^2 distribution.

As the relative frequency discretization $\Delta f/f_p$ increases, f_p becomes more difficult to estimate and hence the pdfs become broader. Whilst n remains small and hence the statistical variability of the spectral estimate dominates over the finite spectral resolution as an error source, the pdfs remain approximately Gaussian. As both $\Delta f/f_p$ and n become significant, the shape of the pdfs become dependent on the specific method used to determine f_p.

As both $\Delta f/f_p$ and n increase, the pdfs for f_p^{max} [Fig. 1(a)] become progressively more "flat-topped" and approximate a uniform distribution. This occurs since the spectral resolution progressively dominates over the statistical variability of the spectrum as an error source and hence this simple estimation technique reproduces the uniform distribution of the discrete frequency grid.

The pdfs for f_p^{D80} [Fig. 1(b)] behave in a similar manner to f_p^{max} as both $\Delta f/f_p$ and n increase. Rather than develop into a simple uniform distribution, they form a uniform distribution with an added narrow peak near f_p. The remaining examples, f_p^{M4} [Fig. 1(c)] and f_p^{PC} [Fig. 1(d)], are even more complex, developing into bi-modal distributions similar to those that could be expected from a sinusoidal wave form. The manner in which such pdfs occur warrants some comment. It is clear from Fig. 1 that these unusual pdfs are caused by the coarse spectral resolution, $\Delta f/f_p$, rather than the statistical variability of the spectrum as they occur when n is large. To investigate this feature a series of realizations of the standard spectrum described earlier were performed with no statistical variability of the spectrum (i.e. $n = \infty$). A value of $\Delta f/f_p = 0.4$ was chosen and the origin for the discrete grid allowed to vary over the interval $\Delta f/f_p$. Rather than vary randomly, however, it was increased in a regular manner. In this manner it is possible to investigate the result as the proximity of a spectral bin to f_p changes. When the closest spectral bin is significantly less than f_p the maximum value of the spectrum is significantly underestimated. As the bin moves closer to f_p, the spectrum becomes "sharper". Hence, the shape of the spectrum and the ability to estimate f_p is critically dependent on the relative positions of f_p and the closest spectral bin.

The consequences of this change in the realized spectral shape on the estimates of $\hat{f}_p$ are shown in Fig. 2. The panels of this figure show f_p^{D80}, f_p^{M4} and f_p^{PC} as functions of the position of the discrete maximum in the spectrum, f_p^{max}. Firstly, consider f_p^{D80}: when the closest spectral bin is distant from f_p, the spectrum is relatively flat and a number of ordinates are included in the average of the values above 80% of the

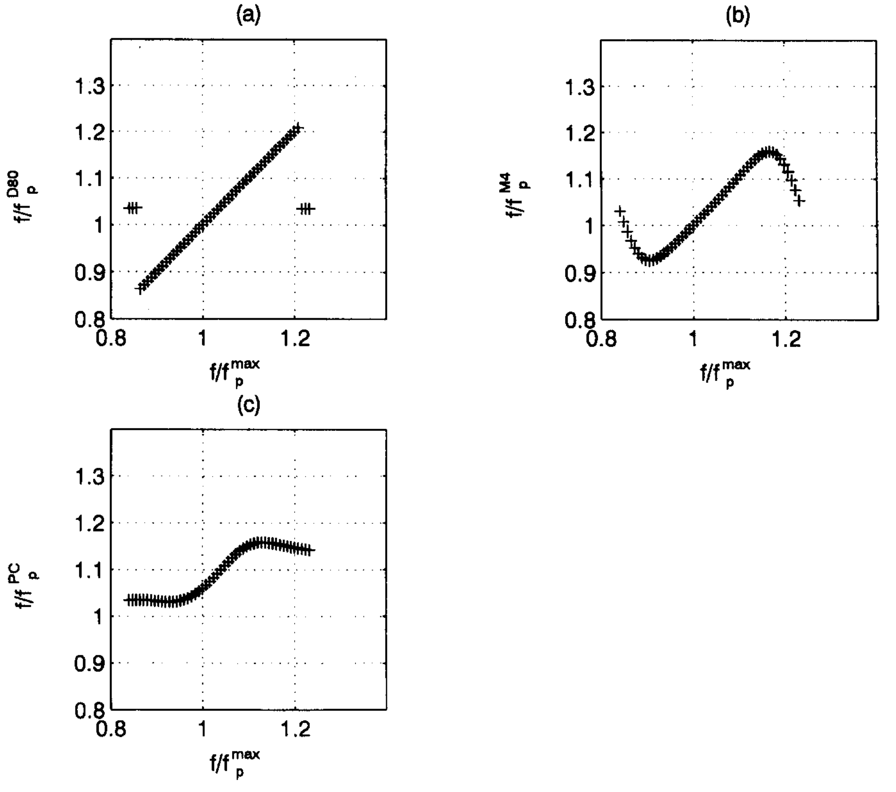

Fig. 2. Comparison of the predicted peak frequency against the frequency of the maximum spectral ordinate. The individual points shown are for frequency grids with differing origin points. The influence of the proximity of a spectral bin to the position of the peak frequency is clear.

maximum value. Despite the poor description of the spectrum, the averaging process produces an estimate of the peak frequency close to unity. As the closest bin approaches f_p, the spectrum becomes more peaked and progressively less ordinates are included in the average. In fact, for the very coarse resolution considered here only one ordinate contributes and hence the technique becomes equivalent to f_p^{max}. This is clearly seen in Fig. 1(a). Hence the resulting pdf is approximately uniform, with an enhancement at $f/f_p \approx 1$. The other two methods produce approximately sinusoidal variations of their respective estimates of the peak frequency as a function of the position of the peak spectral ordinate [Fig. 2(b) and (c)]. Again, this is due to the changing shape of the realized spectrum. As a sinusoid has a bimodal pdf (i.e. more points at crest and trough compared to zero crossing), the pdfs for these techniques become bimodal for both $\Delta f/f_p$ and n large, as observed in Fig. 1.

It is clear from the results of Fig. 1 that it is unlikely that a single analytical form for the pdf for $\hat{f}_p$ could be found. The results do, however, provide a rational method for the intercomparison of the various estimation techniques.

4.3. *Mean values and confidence limits*

Figure 3 shows contour plots of the values of the upper and lower 95% confidence limits as well as the mean values as functions of $\Delta f/f_p$ and n. As previously reported by Donelan and Pierson (1983), all methods overestimate the value of f_p. Also, for all methods, there is little gain in accuracy by increasing n above approximately 50. A detailed quantitative comparison of the various methods will be conducted below; there are, however, a number of features of Fig. 3 that warrant comment. Firstly, $f_p^{\max}$ and f_p^{D80} provide the best estimates of the mean, closely followed by f_p^{M4} with f_p^{PC} significantly overestimating the mean. Although the mean value for $f_p^{\max}$ is close to unity, it has quite broad confidence limits. The narrowest band of confidence limits and hence the "best" estimate of f_p is provided by f_p^{M4}.

A quantitative comparison between the various methods can be made by the definition of error statistics for the full two-dimensional space defined by $\Delta f/f_p$ and n. One such statistic can be defined as

$$\epsilon = \frac{\sum_i \sum_j V_{ij} A_{ij}}{\sum_i \sum_j A_{ij}} \tag{10}$$

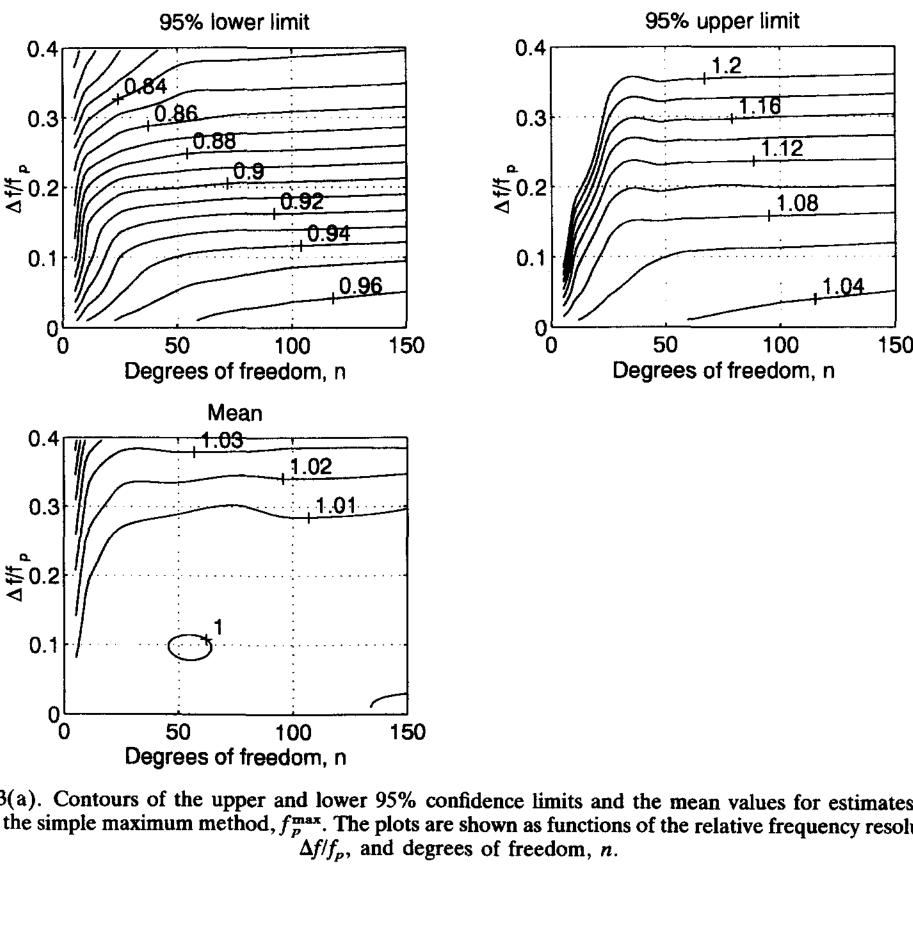

Fig. 3(a). Contours of the upper and lower 95% confidence limits and the mean values for estimates of f_p from the simple maximum method, $f_p^{\max}$. The plots are shown as functions of the relative frequency resolution, $\Delta f/f_p$, and degrees of freedom, n.

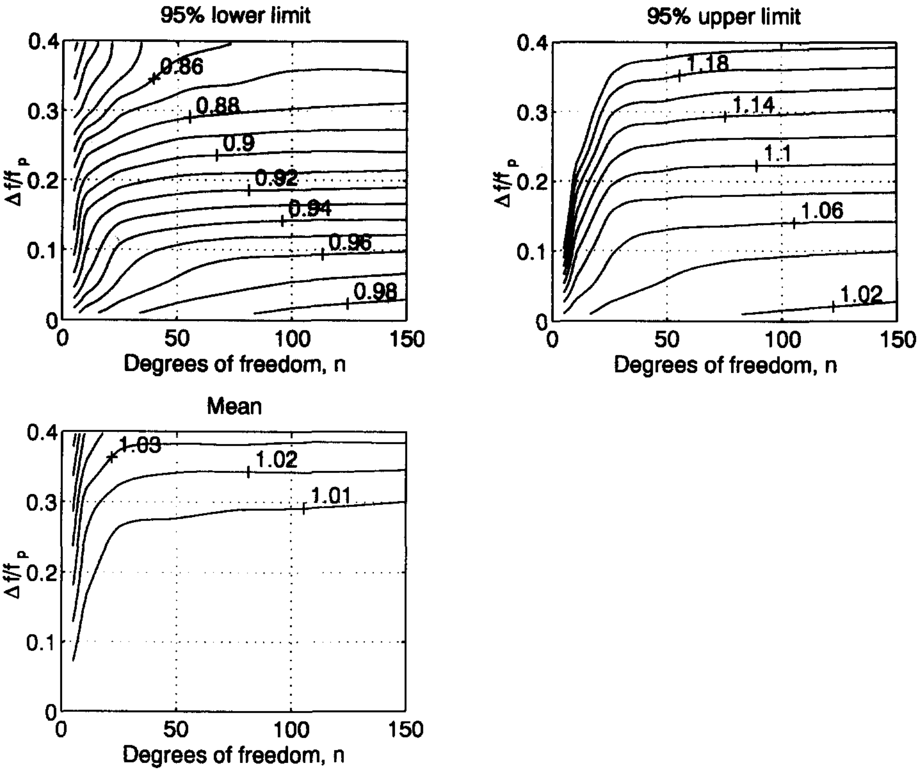

Fig. 3(b). As for Fig. 3(a), but for the "Delft" method, f_p^{D80}.

where V_{ij} could be either the value of the upper or lower 95% confidence limit or the mean, at a point whose corresponding values of $\Delta f/f_p$ and n are defined by the subscripts ij. The summations in (10) range over all 63 values used in the Monte-Carlo simulations as shown in Fig. 3. The non-uniform grid is accounted for by inclusion of the "area" in $\Delta f/f_p$, n space, A_{ij} associated with each value. The results for all the methods investigated are summarised in Table 1.

Most techniques provide similar values for the mean error of approximately 1.01. The one exception is f_p^{PC}, which is biased significantly higher with a value of 1.03. An optimal technique should not only provide a relatively unbiased mean but also a small band for the confidence limits. The difference between the errors for the upper and lower 95% confidence limits is shown in Table 1. The estimate f_p^{PC} provides the smallest value of this quantity, but recall that it also had the largest error for the mean. Of the remaining estimates, f_p^{M4} appears to yield the best overall estimate of f_p with an error difference of 0.157. Not surprisingly, $f_p^{\max}$ produces the largest value for the error difference, confirming the qualitative impression from Fig. 1. As the power is increased in the weighted mean technique (f_p^{M4}–f_p^{M8}) the mean error decreases but the difference error for the confidence limits increases. As the power in this formulation increases, the method approaches the simple maximum $f_p^{\max}$. The identical features are observed as the threshold level is increased in the "Delft" method (i.e. f_p^{D60}–f_p^{D80}).

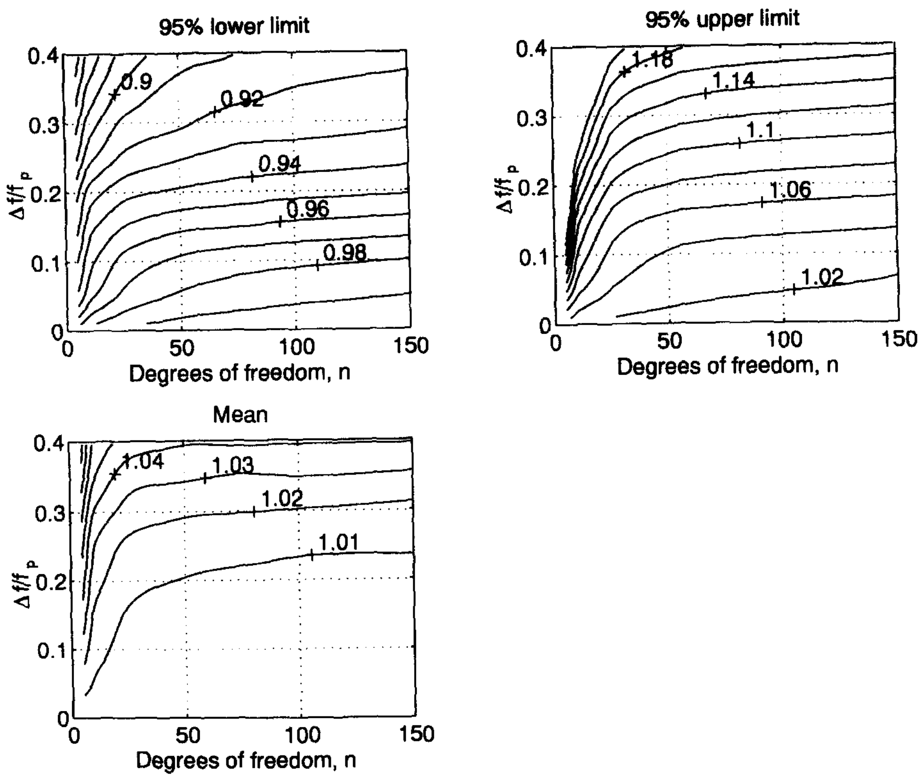

Fig. 3(c). As for Fig. 3(a), but for the weighted mean method, f_p^{M4}.

In summary, it can be concluded that of the techniques investigated, f_p^{M4} provides the most reliable estimate of f_p.

4.4. *Spectral peakedness*

In the analysis performed above, the spectral peakedness has been held constant at $\gamma = 3$. As already pointed out by Bishop and Donelan (1988), γ plays an important role in the accuracy with which f_p can be estimated. A peaked spectrum with a large value of γ will have less error associated with the estimate of f_p than a flatter spectrum with a small value of γ. To investigate the influence of γ in the determination of f_p two further Monte-Carlo simulations were performed. The f_p^{M4} method was used; however, γ was changed from the original value of 3 to 1 and 7, respectively. The error values are summarised in Table 1. As expected, decreasing γ increases both the mean error and also the confidence limit difference error. There is more error associated with estimates of f_p for a spectrum with $\gamma = 1$ than for a spectrum with $\gamma = 3$. As γ increases above 3, the error values continue to decrease, but not significantly. This indicates that there is little increase in the error beyond $\gamma = 3$.

The results of the Monte-Carlo simulations provide a practical and easily implemented means for the estimation of confidence limits for f_p. The Appendix contains the tabulated values for the simulations of f_p^{M4} for $\gamma = 1$, 3 and 7. Intermediate values can be obtained with reasonable accuracy by interpolation.

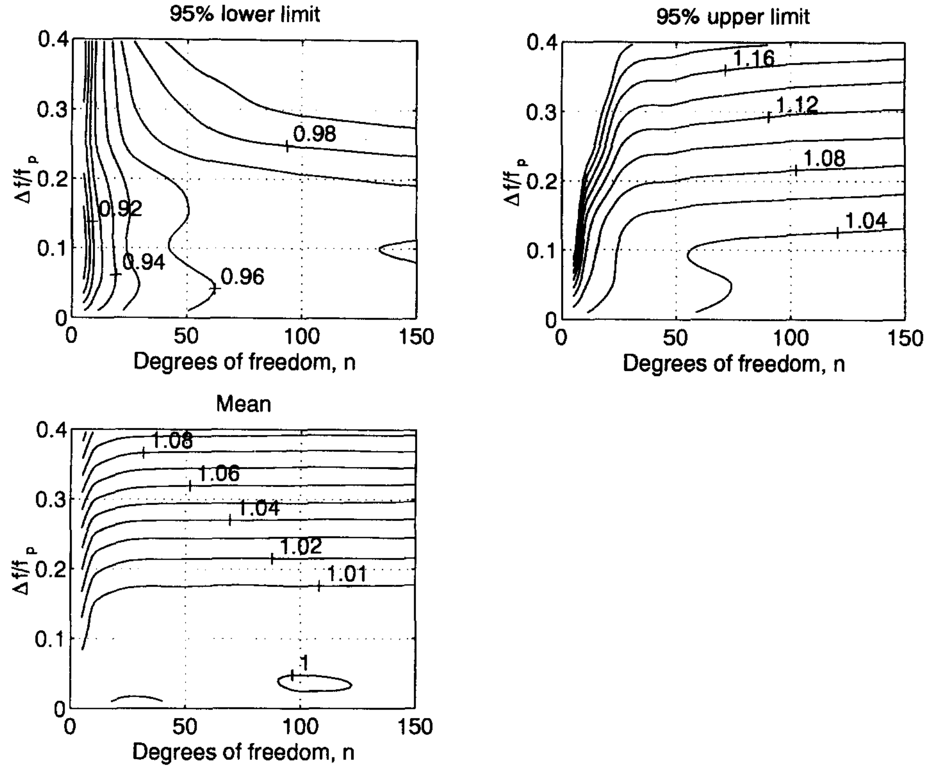

Fig. 3(d). As for Fig. 3(a), but for the peak centroid method, f_p^{PC}.

Table 1. Values of ϵ for each of the estimation methods

Estimate	95% lower limit	95% upper limit	Difference upper–lower	Mean
f_p^{max}	0.8937	1.1367	0.2430	1.0105
f_p^{D60}	0.9270	1.1071	0.1802	1.0136
f_p^{D80}	0.9091	1.1182	0.2091	1.0107
f_p^{M4}	0.9432	1.1002	0.1570	1.0173
f_p^{M5}	0.9335	1.1012	0.1677	1.0136
f_p^{M8}	0.9194	1.1090	0.1896	1.0110
f_p^{PC}	0.9723	1.1071	0.1348	1.0334
f_p^{S}	0.9198	1.0997	0.1798	1.0080
f_p^{M4} $\gamma = 1$	0.9782	1.1685	0.1903	1.0723
f_p^{M4} $\gamma = 7$	0.9338	1.0925	0.1587	1.0100

5. CONCLUSIONS

The Monte-Carlo simulations performed have shown a number of interesting features of the statistical variability of estimates of the spectral peak frequency. Probability density functions of $\hat{f}_p$ and hence confidence limits are clearly functions of both the relative spectral resolution, $\Delta f/f_p$, and the number of degrees of freedom of the spectral estimate, n.

A number of proposed techniques for the estimation of f_p have been investigated. All methods produce estimates of the peak frequency with means greater than the true value. The method which produces the smallest confidence band for $\hat{f}_p$ is the weighted mean method of Sobey and Young (1986) and Reid (1986), but with a weighting exponent of 4 (i.e. f_p^{M4}).

Not surprisingly the spectral peakedness, as measured by the peak enhancement factor γ, also determines the accuracy with which f_p can be estimated. The error increases as the spectral peakedness decreases.

Tabular results have been presented in the Appendix which enable the mean bias as well as 95% confidence limits to be determined with knowledge of $\Delta f/f_p$, n and γ. These tables provide a practical manner in which to assign confidence limits to estimates of f_p.

REFERENCES

Bendat, J.S. and Piersol, A.G. 1971. *Random Data: Analysis and Measurement Procedures*. Wiley-Interscience, New York (407 pp.).

Bishop, C.T. and Donelan, M.A. 1988. Waves and wave forecasting. In *Civil Engineering Practice 3—Geotechnical/Ocean Engineering*, pp. 653–695. Technomic, Lancaster, PA.

Donelan, M.A., Hamilton, J. and Hui, W.H. 1985. Directional spectra of wind-generated waves. *Phil. Trans. R. Soc. Lond. A* **315**, 509–562.

Donelan, M.A. and Pierson, W.J. 1983. The sampling variability of estimates of spectra of wind-generated gravity waves. *J. Geophys. Res.* **88**, 4381–4392.

Günther, H. 1981. A parametric surface wave model and statistics of the prediction parameters. *Hamburger Geophys. Einzelsch.* **55**, 1–90.

IAHR/PIANC 1986. *List of Sea State Parameters*. PIANC Supplement to Bulletin No. 52, General Secretariat of Pianc, Brussels.

Mansard, E.P.D. and Funke, E.R. 1988. On the fitting of parametric models to measured wave spectra. In *Proceedings of the 2nd International Symposium on Waves and Coastal Engineering, Hannover, Germany*.

Mansard, E.P.D. and Funke, E.R. 1990. On fitting of JONSWAP spectra to measured sea states. In *Proceedings of the 22nd International Coastal Engineering Conference, Delft, The Netherlands*, pp. 465–477.

Read, W.W. 1986. Time series analysis of wave records and the search for wave groups. Ph.D. thesis, James Cook University of North Queensland, Australia.

Sobey, R.J. and Young, I.R. 1986. Hurricane wind waves—a discrete spectral model. *ASCE J. WatWay, Port, Coastal Ocean Engng* **112**, 370–389.

Young, I.R. 1986. Probability distribution of spectral integrals. *ASCE J. WatWay, Port, Coastal Ocean Engng* **112**, 338–341.

APPENDIX

$\downarrow$ $\Delta f/f_p$, $n \rightarrow$	Mean values, $\gamma = 1$						
	5	10	25	50	75	100	150
0.40	1.1436	1.1112	1.0909	1.0818	1.0780	1.0757	1.0742
0.35	1.1374	1.1095	1.0867	1.0771	1.0734	1.0714	1.0699
0.30	1.1320	1.1053	1.0836	1.0743	1.0721	1.0696	1.0674
0.25	1.1214	1.0987	1.0801	1.0719	1.0692	1.0674	1.0657
0.20	1.1142	1.0943	1.0774	1.0701	1.0680	1.0672	1.0652
0.15	1.1079	1.0883	1.0740	1.0684	1.0662	1.0656	1.0650
0.10	1.0951	1.0831	1.0718	1.0671	1.0659	1.0647	1.0638
0.05	1.0843	1.0740	1.0676	1.0650	1.0643	1.0638	1.0633
0.01	1.0695	1.0657	1.0636	1.0630	1.0628	1.0629	1.0630

$\downarrow$ $\Delta f/f_p$, $n \rightarrow$	Lower 95% confidence limit, $\gamma = 1$						
	5	10	25	50	75	100	150
0.40	0.8510	0.8718	0.9118	0.9314	0.9392	0.9470	0.9570
0.35	0.8597	0.8885	0.9190	0.9403	0.9523	0.9606	0.9713
0.30	0.8697	0.8945	0.9290	0.9495	0.9655	0.9724	0.9829
0.25	0.8773	0.9007	0.9382	0.9632	0.9768	0.9842	0.9950
0.20	0.8877	0.9179	0.9516	0.9724	0.9864	0.9956	1.0079
0.15	0.8979	0.9241	0.9590	0.9843	0.9963	1.0051	1.0149
0.10	0.9086	0.9383	0.9744	0.9944	1.0071	1.0136	1.0218
0.05	0.9308	0.9608	0.9944	1.0113	1.0206	1.0263	1.0334
0.01	0.9788	1.0022	1.0269	1.0381	1.0430	1.0459	1.0493

$\downarrow$ $\Delta f/f_p$, $n \rightarrow$	Upper 95% confidence limit, $\gamma = 1$						
	5	10	25	50	75	100	150
0.40	1.5441	1.4203	1.2753	1.2142	1.1913	1.1832	1.1743
0.35	1.5255	1.3855	1.2668	1.2050	1.1782	1.1645	1.1512
0.30	1.4913	1.3646	1.2580	1.2011	1.1716	1.1574	1.1381
0.25	1.4524	1.3369	1.2390	1.1891	1.1625	1.1504	1.1335
0.20	1.4173	1.3122	1.2231	1.1709	1.1511	1.1401	1.1242
0.15	1.3773	1.2849	1.1994	1.1590	1.1392	1.1282	1.1166
0.10	1.3230	1.2532	1.1770	1.1411	1.1269	1.1166	1.1069
0.05	1.2605	1.1996	1.1440	1.1189	1.1081	1.1011	1.0934
0.01	1.1640	1.1282	1.1002	1.0875	1.0828	1.0798	1.0767

	Mean values, $\gamma = 3$						
$\downarrow \Delta f/f_p$, $n \rightarrow$	5	10	25	50	75	100	150
0.40	1.0864	1.0600	1.0469	1.0413	1.0420	1.0412	1.0412
0.35	1.0754	1.0512	1.0346	1.0317	1.0294	1.0303	1.0287
0.30	1.0630	1.0395	1.0263	1.0215	1.0204	1.0195	1.0175
0.25	1.0527	1.0301	1.0175	1.0143	1.0131	1.0115	1.0114
0.20	1.0446	1.0246	1.0129	1.0097	1.0083	1.0082	1.0073
0.15	1.0359	1.0176	1.0091	1.0068	1.0054	1.0056	1.0050
0.10	1.0250	1.0132	1.0071	1.0053	1.0045	1.0044	1.0037
0.05	1.0137	1.0088	1.0054	1.0044	1.0041	1.0039	1.0037
0.01	1.0059	1.0046	1.0038	1.0037	1.0036	1.0037	1.0036

	Lower 95% confidence limit, $\gamma = 3$						
$\downarrow \Delta f/f_p$, $n \rightarrow$	5	10	25	50	75	100	150
0.40	0.8524	0.8711	0.8924	0.9054	0.9097	0.9139	0.9168
0.35	0.8644	0.8816	0.9014	0.9127	0.9159	0.9200	0.9227
0.30	0.8762	0.8938	0.9116	0.9182	0.9244	0.9257	0.9283
0.25	0.8889	0.9065	0.9218	0.9289	0.9333	0.9345	0.9372
0.20	0.9068	0.9237	0.9363	0.9416	0.9445	0.9465	0.9485
0.15	0.9171	0.9366	0.9502	0.9578	0.9597	0.9624	0.9647
0.10	0.9300	0.9472	0.9636	0.9720	0.9760	0.9778	0.9803
0.05	0.9427	0.9579	0.9728	0.9814	0.9845	0.9871	0.9900
0.01	0.9681	0.9782	0.9877	0.9923	0.9947	0.9959	0.9971

	Upper 95% confidence limit, $\gamma = 3$						
$\downarrow \Delta f/f_p$, $n \rightarrow$	5	10	25	50	75	100	150
0.40	1.4913	1.3175	1.2164	1.1862	1.1792	1.1737	1.1689
0.35	1.4353	1.2923	1.1859	1.1573	1.1484	1.1451	1.1402
0.30	1.3895	1.2456	1.1557	1.1306	1.1224	1.1184	1.1137
0.25	1.3421	1.2085	1.1282	1.1031	1.0969	1.0938	1.0903
0.20	1.3009	1.1689	1.0988	1.0798	1.0743	1.0713	1.0680
0.15	1.2435	1.1285	1.0728	1.0556	1.0519	1.0491	1.0460
0.10	1.1790	1.0977	0.0546	1.0383	1.0328	1.0306	1.0266
0.05	1.1039	1.0651	1.0391	1.0286	1.0236	1.0211	1.0174
0.01	1.0450	1.0315	1.0205	1.0151	1.0128	1.0115	1.0099

↓ $\Delta f/f_p$, n →	Mean values, $\gamma = 7$						
	5	10	25	50	75	100	150
0.40	1.0643	1.0479	1.0371	1.0343	1.0351	1.0327	1.0333
0.35	1.0520	1.0360	1.0246	1.0219	1.0216	1.0206	1.0199
0.30	1.0376	1.0216	1.0150	1.0133	1.0117	1.0116	1.0099
0.25	1.0267	1.0133	1.0068	1.0071	1.0062	1.0047	1.0049
0.20	1.0187	1.0072	1.0033	1.0025	1.0024	1.0022	1.0018
0.15	1.0110	1.0028	1.0011	1.0012	1.0009	1.0008	1.0010
0.10	1.0054	1.0017	1.0004	1.0006	1.0007	1.0004	1.0001
0.05	1.0016	1.0009	1.0007	1.0003	1.0005	1.0003	1.0003
0.01	1.0006	1.0005	1.0004	1.0003	1.0003	1.0003	1.0003

↓ $\Delta f/f_p$, n →	Lower 95% confidence limit, $\gamma = 7$						
	5	10	25	50	75	100	150
0.40	0.8481	0.8705	0.8855	0.8940	0.8978	0.8991	0.9017
0.35	0.8611	0.8780	0.8923	0.9005	0.9027	0.9043	0.9064
0.30	0.8751	0.8887	0.9021	0.9061	0.9087	0.9101	0.9113
0.25	0.8951	0.9028	0.9119	0.9169	0.9187	0.9191	0.9201
0.20	0.9124	0.9206	0.9276	0.9303	0.9324	0.9330	0.9339
0.15	0.9264	0.9361	0.9448	0.9487	0.9500	0.9510	0.9517
0.10	0.9375	0.9515	0.9630	0.9679	0.9702	0.9716	0.9728
0.05	0.9499	0.9620	0.9747	0.9809	0.9843	0.9859	0.9884
0.01	0.9711	0.9790	0.9868	0.9908	0.9926	0.9938	0.9948

↓ $\Delta f/f_p$, n →	Upper 95% confidence limit, $\gamma = 7$						
	5	10	25	50	75	100	150
0.40	1.4532	1.2802	1.2051	1.1827	1.1770	1.1717	1.1686
0.35	1.3995	1.2469	1.1734	1.1514	1.1463	1.1432	1.1391
0.30	1.3294	1.1900	1.1368	1.1232	1.1190	1.1172	1.1145
0.25	1.2651	1.1461	1.1079	1.0984	1.0955	1.0945	1.0929
0.20	1.1987	1.1042	1.0817	1.0757	1.0742	1.0729	1.0711
0.15	1.1268	1.0709	1.0578	1.0535	1.0522	1.0508	1.0503
0.10	1.0841	1.0527	1.0384	1.0332	1.0309	1.0294	1.0278
0.05	1.0553	1.0403	1.0270	1.0197	1.0165	1.0148	1.0122
0.01	1.0306	1.0224	1.0140	1.0100	1.0080	1.0070	1.0058